Fluid Dynamics, Vol. 35, No. 4, 2000

EXPERIMENTAL INVESTIGATION OF THE INTERACTION BETWEEN AN ELECTRICALLY CHARGED LIQUID-DROP DISPERSED PHASE AND A TURBULENT AIR-STEAM JET

A. B. Vatazhin, V. A. Likhter, and V. I. Shul'gin

UDC 532.529:532.525.2:537.532.3

The interaction of an electrically charged liquid-drop dispersed phase with a turbulent air-steam jet in a "water drop generator (capillary)-jet-target" system is investigated. The experimental conditions were as follows: volume flow of water through the capillary 0.01 cm^3/s, capillary inside diameter 0.8 mm, electric potential applied to the capillary 20 kV. When the electric field is absent, condensation does not develop in the jet despite the existence of oversaturation zones. Two regimes of interaction between the charged dispersed phase and the jet are detected. The first regime (for $\varphi < 8$ kV) is characterized by the regular launching of fairly large charged drops ($0.5 < r < 2$ mm) from the capillary and the absence of condensation in the jet. As the potential φ increases, the drop size decreases, whereas the drop charge increases. This regime made it possible to model the motion of individual charged clusters of different charge and size in aircraft engine jets. The second regime ($\varphi > 8$ kV) is characterized by the irregular launching of drops from the capillary, drop dispersion with respect to size, a sharp increase in the target current, and the sudden appearance of condensation in the air-steam jet. The possible electrohydrodynamic and heterophase processes are qualitatively analyzed.

There has recently been much interest in the problem of using electric effects in engine gas flows for flow diagnostics and the analysis of engine component performance. One aspect of this problem is the method of contactless electrostatic aircraft jet engine diagnostics [1]. The theoretical basis for the modification of the method used by the authors was given in [2]. The first airfield tests have already been carried out under the contactless electrostatic diagnostics program for modern aircraft engines. In some cases, in time realizations of the electric signal from the test aircraft's engine jet individual segments can be distinguished, which, according to the theory [2], can be regarded as an electric "response" to the motion of individual clusters of charged particles. The cluster charge is of the order of 10^{-11}–10^{-12} C.

To register these charged clusters and analyze their motion in turbulent jets, bench modeling is required, the basic elements being the turbulent air-steam jet and large particles with the above-mentioned charge.

The present study is devoted to such modeling and the description and qualitative analysis of the results obtained.

In the bench experiments, as the large charged particles we used water drops 0.5–2 mm in size, which were created at the capillary end in a special charged drop generator. In most experiments, the drop generator and the nozzle, from which the steam flowed, had the same potential. The case of the grounded nozzle will be considered separately. Two regimes of drop generator operation were detected. The first regime, with a regular succession of drops, which enter the jet, are entrained in the motion and registered by a special probe mounted downstream, is realized for $\varphi < 8$ kV. The second, with a sharp increase in the electric current from the capillary, irregular motion of the drops, and the appearance of a long condensation zone in the air-steam jet, is realized for $\varphi > 8$ kV (for $\varphi < 8$ kV, no condensation in the jet is observed). Below, this unusual situation is analyzed qualitatively.

1. EXPERIMENTAL SET-UP

The scheme of the experimental setup is shown in Fig. 1. The steam jet flows from nozzle *1* into the surrounding air. The experimental system of air-steam jet generation for various temperature conditions was described in [3]. The charged drops are created in an electrically isolated capillary system which is under the electric potential φ ($|\varphi| \le 20$ kV). The capillary system consists of a vessel *2* filled with water ($H = 190$ mm) and a capillary *3* formed by a spiral stainless-steel tube of length $l = 1.5$ m ($h = 200$ mm). The outside and inside tube diameters are 1 mm and 0.8 mm, respectively.

The drop succession frequency was determined using the signal of a photodiode, at which a laser beam 1 mm in diameter intersecting the falling drop trajectory was directed (in Fig. 1, the laser system is not shown).

The falling drop parameters were determined in the absence of a jet. In this case, the drops traveled a vertical distance Y to a horizontally oriented target *4* grounded across the circuit formed by the amplifier *7* and oscillograph *8*, used for registering the electric current of the drops.

Moscow, e-mail: vatazhin@ciam.ru, likhter@ciam.ru. Translated from Izvestiya Rossiiskoi Akademii Nauk, Mekhanika Zhidkosti i Gaza, No. 4, pp. 102–114, July–August, 2000. Original article submitted November 29, 1999.

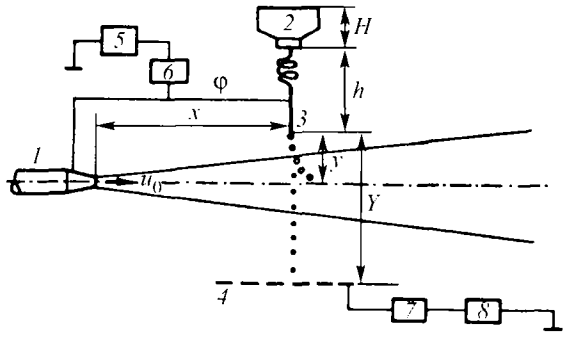

Fig. 1. Scheme of the experimental setup.

The drop volume flow rate G was measured by collecting the falling drops in a special vessel over a fixed, fairly long time interval, on which, however, the height H in vessel 2 changed only slightly.

The drop fall velocity at a certain point between the capillary and the target was determined by registering the signals from two laser beams passing one higher and one lower in the neighborhood of that point. The charge on a drop Q was determined by integrating the electric signal from the drop on oscillograph 8 (Fig. 1).

2. EXPERIMENTAL RESULTS. REGIME I

Firstly, we will consider the regime realized for $0 < \varphi < 8$ kV and characterized by a regular succession of charged drops.

An important experimental result is the only slight dependence of the flow rate G on the capillary potential φ for $\varphi < 6$ kV. To explain this result, we will theoretically estimate the value of the fluid flow rate in the drop generator. In the capillary tube, the flow is laminar with a Reynolds number ≈ 16. In the tube, the initial hydrodynamic section length equal to several tube calibers, is three orders smaller than the total tube length. The tube diameter is much smaller than the radius of its spiral loop (see Fig. 1) and the secondary effects in the tube flow are insignificant. Taking all this into account, for tube sections we can use the Poiseuille formula relating the local pressure gradient with the fluid flow rate. Including the gravity force in this formula and integrating over the entire tube length, with account for the boundary conditions for the pressure at the tube inlet and outlet we obtain:

$$G=\frac{\pi d^4 \rho g(H + h)(1 + A)}{128 \mu l}, \qquad A=\frac{(E_*^2/8\pi) - (2\alpha/r_*)}{\rho g(H + h)} \tag{2.1}$$

Here, $d=0.8$ mm is the capillary diameter, μ is the "effective" dynamic viscosity of the water inside the capillary tube (which takes into account the possible roughness of the inner tube surface and can exceed the standard value $\mu=10^{-2}$ g/(cm·s)), ρ is the water density, g is the gravity force acceleration, $\alpha=72$ g/s^2 is the water surface tension coefficient, and r_* and E_* are the effective values of the linear scale and the electric field used for calculating the surface tension pressure and the electric pressure near the bottom point of a drop located on the capillary end. Assuming for estimating purposes $r=0.5$ mm and $E_*=\varphi/r_*$, we find that, for regimes with $\varphi < 4$ kV, on the drop end the surface tension predominates, whereas, for high φ, the main contribution to the value of A is made by the electric pressure. For $\varphi < 6$ kV, the value of A is not large ($A < 0.09$). This explains the aforementioned experimental observation.

The arithmetic mean of the flow rate is $G=0.01$ cm^3·s^{-1}. This is ten times greater than the fluid flow rate in studies [4–6], in which the process of electric spraying into small monodisperse drops in the "Taylor cone" regime was investigated. Precisely this relatively large value of G made it possible to solve the experimental problem, namely, to create a regime with coarse, electrically charged drops.

The drop radius was determined from the relation $G=(4/3)\pi r^3 f$, where f is the drop succession frequency. Since G depends only slightly on φ, the drop succession frequency and the drop size are related by an approximate formula $r^3 f=r_0^3 f_0$, where the subscript 0 corresponds to the regime with $\varphi=0$.

The experimental values of the charge Q, the size r, and the frequency f of single drops for various φ, and also the values of the electric field intensity on the drop surface, calculated using the formula $E=Q/r^2$, are given in Table 1.

TABLE 1

$\|\varphi\|$, kV	f, s^{-1}	Q, C	r, cm	E, W/cm
0	0.50		0.170	
2	0.57	$5.0 \cdot 10^{-12}$	0.162	171.5
3	0.61	$5.7 \cdot 10^{-12}$	0.159	202.9
3.5	0.63	$8.8 \cdot 10^{-12}$	0.157	321.3
4	0.66	$9.0 \cdot 10^{-12}$	0.155	337.1
5	0.98	$8.0 \cdot 10^{-12}$	0.136	425.3
6	4.82	$6.9 \cdot 10^{-12}$	0.080	970.3

Table 1 shows the experimental results for φ corresponding to the regular regimes of drop formation and motion.

According to Table 1, the drop succession frequency increases with increase in the potential. This can be explained as follows. As φ increases, the electric field on the drop formed on the capillary end increases. The electric pressure, proportional to the square of the electric field and directed along the outward normal to the fluid surface, also increases. This leads to a decrease in the effective surface tension and, under the action of the gravity force, the drops of smaller radius are detached.

We also note that, for $\varphi < 6$ kV, the drop size is noticeably greater than the capillary inside diameter.

To estimate the development of the instability on the drop surface, we will use the maximum value of the drop charge Q_m (such that, if it is exceeded, the Rayleigh instability [7] develops) and the critical external field E_∞ (such that, if it is exceeded, cusps with the ejection of small fluid jets are formed on the drop surface [4, 8]). These critical values are given by the formulas:

$$Q_m=(16\pi\alpha r^3)^{1/2}, \qquad E_\infty=(2.6\alpha/r)^{1/2} \tag{2.2}$$

It is also necessary to use information on the electric field E_* of ignition of the corona discharge from the drop surface. If, as the first approximation, we assume that the E_* for the water drop is equal to that for a spherical metal particle of the same radius, then, according to [9, 10], for all drop sizes given in Table 1 we have: $70 \le E_* \le 80$ kV/cm.

Using this information, we can conclude that on the detached drops the field E is much smaller than E_* (no corona displayed on the drops) and the drop charge Q is two or three orders of magnitude smaller than the maximum charge Q_m. Moreover, at the drop location points (see Sec. 4), except for a small region near the capillary end, the external field E (in the capillary-target system) is much smaller than the critical field E_∞ and the drops do not deform according to the Taylor mechanism. However, near the capillary end Taylor cusps may develop on large drops.

A specific feature of the results in Table 1 is the only slight dependence of the drop radius r on the applied potential for $0 \le \varphi \le 5$ kV. We will give the simplest explanation for this.

The system of governing parameters (we will call it the S system) for the process of drop formation on the capillary end in the regime considered includes the quantities: ρg, α, $b=d/2$, φ, and G. We assume that the fluid is perfectly conducting and that viscous effects are insignificant. The density ρ does not enter into the S system due to the low inertia of the drop growth on the capillary end. The S system must also include the nondimensional constants and the functions describing the experimental system geometry.

By means of similarity and dimensionality theory, we obtain the following relations:

$$r=bf(K, \beta), \qquad r_0=bf(K, 0)$$

$$\frac{r}{r_0}=\frac{f(K, \beta)}{f(K, 0)}=F(K, \beta), \qquad K=\frac{4\alpha}{\rho g b^2}, \qquad \beta=\frac{\varphi^2}{8\pi\rho g b^3}$$

Here, r_0 is the drop radius for $\varphi=0$. In the experiment, the parameter K is constant, whereas the parameter β is varied. If the water viscosity were taken into account, the system of nondimensional parameters would also include the quantity $\mu G/\rho g b^4$. For our experimental conditions it is less than 0.02, which made it possible to neglect the viscous effects.

To obtain the simplest estimate of the size of the drops launched from the capillary, we will consider the following model. Let a drop on the capillary end just before the onset of its sharp deformation and subsequent detachment have the shape of a spherical segment of radius r resting on the capillary exit section.

In regime I, $r > b$ and the segment volume is approximately equal to $(4/3)\pi r^3$. We assume that the quantity E^2 (here, E is the electric field normal to the drop surface and directed outward from the segment) is constant on the segment surface. Assuming realization of the state in which the sum of the projections of the surface tension and the surface electrostatic

forces on the vertical gravity force axis is zero, we obtain the following condition:

$$\left(\frac{2\alpha}{r} - \frac{E^2}{8\pi}\right)\pi b^2 = \frac{4}{3}\pi r^3 \rho g \tag{2.3}$$

By assuming that $E = \varphi/r$, after simple calculations we obtain the following equation:

$$z - z^5 = \beta^*, \quad r = Az, \quad A = 0.5b(6K)^{1/4}, \quad \beta^* = \frac{4\beta}{6^{1/4}K^{5/4}} \tag{2.4}$$

In the absence of an electric field, only the root $z = 1$ is physically meaningful and, hence, $r_0 = A$. For the experimental conditions, $K = 118$ and $r_0 = A = 0.13$ cm. The calculated value of r_0 differs from that given in Table 1 by approximately 20%.

On the range $\varphi = 0$–4 kV, the parameter β^* is small (for $\varphi = 4$ kV it is equal to 0.38). An approximate solution of Eq. (2.4), correct to the terms of the order of $(\beta^*)^2$, has the form:

$$r = r_0(1 - 0.25\beta^*) \quad (\varphi < 4 \text{ kV}) \tag{2.5}$$

This shows that the ratio r/r_0 decreases by not more than 10%, which agrees with the data from Table 1.

The model (2.3) is very approximate. In reality, the drop shape on the capillary end is not spherical, on the drop surface $E^2 \neq \text{const}$, and the condition $E = \varphi/r$ is satisfied only approximately near the drop bottom point. In general, it is necessary to consider a complex electrogasdynamical problem of drop formation and detachment with account for the relations between the parameters on the drop surface as on a surface of discontinuity. However, even the approximate model used made it possible to explain and even quantitatively reproduce the characteristics obtained experimentally for small values of the electric potential. (We note that a force balance equation like (2.3) is widely used for approximate estimates in many publications).

3. EXPERIMENTAL RESULTS. REGIME II

For $8 < \varphi < 15$ kV, the interaction between the electrically charged drops and the turbulent steam-air jet has some interesting and unexpected features. To make them clearer, we will consider in turn the situations with and without the jet.

The analysis of the regimes in the absence of a jet is aimed at clarifying the specific features of the formation and motion of the charged drops in the working section between capillary *3* and target *4* (Fig. 1). It is an electrogasdynamical problem with a voluminous bibliography. This problem was first considered in connection with the problem of using an electric field to produce a monodisperse aerosol. We will mention only two trends in these studies. For relatively small capillary fluid mass flows, the EHD drop spraying regime with the formation of a "Taylor cone" was first studied theoretically in [4]. In [5], the EHD spraying of various fluids was investigated experimentally, the similarity relations and an extensive bibliography are given. EHD spraying with Taylor cone formation was analyzed theoretically in [6]. The regime of EHD-spraying in a strong electric field for fairly high fluid flows, with the formation of rotating fluid jets launched from the capillary and then fragmenting into small drops, was investigated in [11].

In the present study, the chosen value of the fluid flow and the range of variation of the electric potential (necessary for modeling the motion of discrete charged clusters in turbulent jets) differ from those used in the studies mentioned above and are characterized by a number of specific features briefly discussed below.

When the electric potential is varied on the range 8–10 kV, the regular regime of succession of approximately equal drops ceases to exist. By measuring the time intervals Δt between the successive traverses of the laser beam by drops of different size and assuming that the values of Δt differ only slightly from the corresponding time intervals for the capillary end, for given experimental values of the capillary fluid flow we can determine the diameter of the detached drops. We observed regimes characterized by the formation of mainly two drop fractions with sizes $\approx$0.5 and 0.2 mm. For other experimental conditions, the formation of one large drop followed by several small drops was considered in [12].

The situation changes radically if the potential lies on the range $\varphi = 11$–15 kV. The drops no longer regularly cross the laser beam. Videophotography of the spraying shows that the detached drops move inside a cone whose apex coincides with the capillary end, while the aperture angle increases with increase in the voltage (Fig. 2). The continuous curves shown in Fig. 2 are not liquid jets. Since the videophotography exposure time is fairly large (0.02 s), these curves are the trajectories of individual particles. We also carried out videophotography with a much smaller exposure time (0.002 s) and images with clearly expressed charged-drop "traces" were obtained; the trace length being equal to the distance traveled by the drop during exposure (Fig. 3).

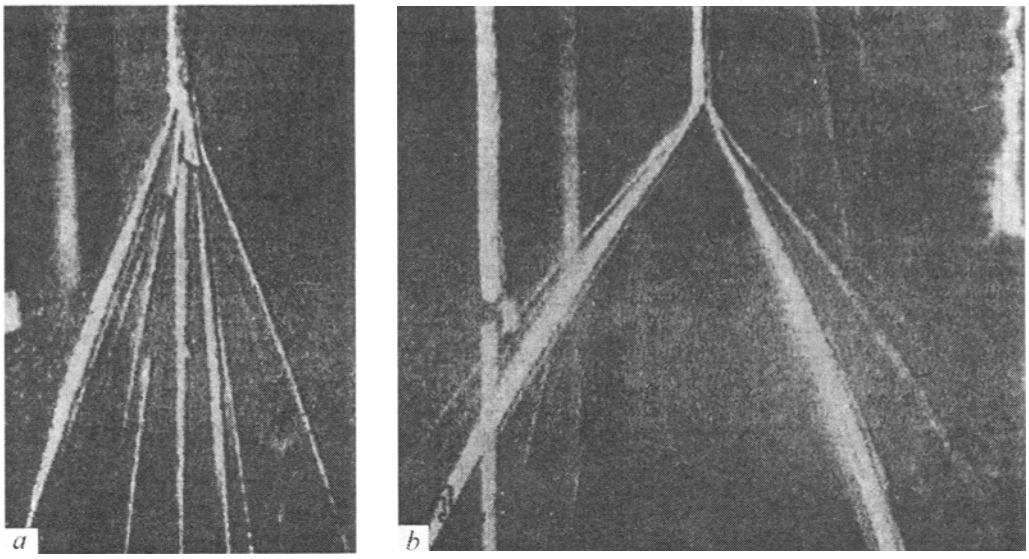

Fig. 2. Stop-image obtained by continuous videophotography (exposure 0.02 s) of drop spraying from the capillary end under high electric potential. *a*: $\varphi = 12$ kV, *b*: $\varphi = 15$ kV. The continuous curves show the trajectories of the individual drops.

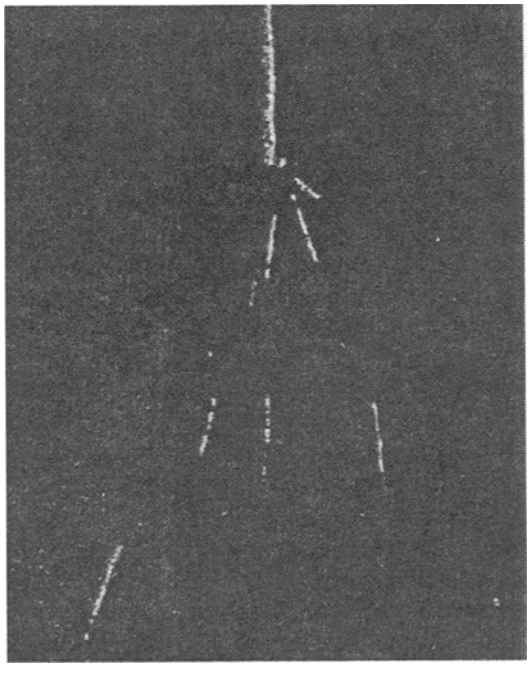

Fig. 3. Stop-image obtained by short-exposure (0.002 s) videophotography of drop spraying from the capillary end for $\varphi = 15$ kV. The segments of continuous curves show the traces of individual drops.

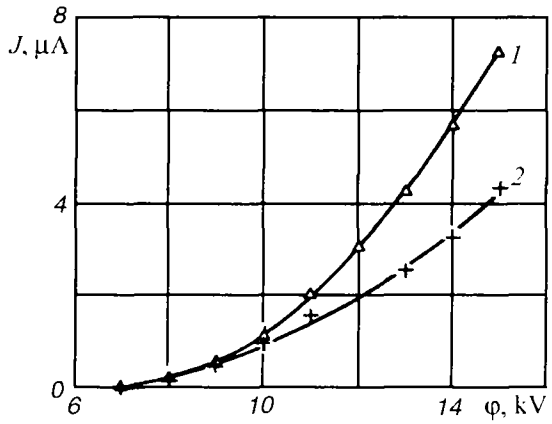

Fig. 4

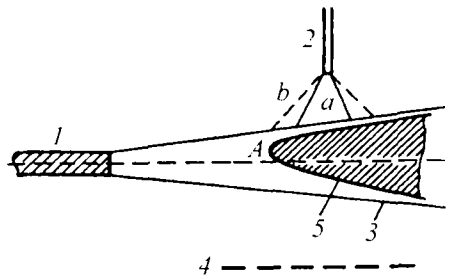

Fig. 5

Fig. 4. Volt-ampere characteristics of the "capillary-target" system in the absence (curve *1*) and presence of an air-steam jet with the development of condensation after the introduction of charged drops (curve *2*).

Fig. 5. Condensation zone location in the turbulent air-steam jet with the introduction of charged drops for $8 < \varphi < 15$ kV.

The volt-ampere characteristic of the process, namely, the electric current J on the target grounded through a microamperemeter as a function of the potential difference applied to the capillary in the absence of an air-steam jet φ, is presented in Fig. 4 (curve *1*). For $\varphi < 8$ kV (regime I) the current J is very small. It becomes noticeable when φ varies on the range 8–10 kV and, for greater φ, increases sharply.

We will now consider the experimental results for the "capillary-air-steam jet (steam outflow into the ambient space)-target" system. The experiments were performed for the following air-steam jet parameters: steam nozzle diameter 2.8 mm, temperature of the ambient air $T_\infty = 15°C$, steam temperature at the nozzle outlet $T_0 = 102°C$ (steam oversaturation regions exist in the jet), and steam velocity at the nozzle outlet 200 m/s. The capillary was located in a section $x = 5$ cm outside the jet at a distance of 2.5 cm from the jet axis.

In regime I ($\varphi < 8$ kV), when the drops enter the jet there is no condensation ($T_0 = 102°C$). However, in regime II ($\varphi > 8$ kV) an unexpected situation arises, namely, a region of intense condensation, shown schematically in Fig. 5, develops in the jet. It was visualized in the "laser light sheet" plane. In the same figure, the conic regions occupied by the charged drops and located above the jet are shown for $\varphi = 12$ kV (*a*) and 15 kV (*b*).

The volt-ampere characteristic in the "capillary-jet ($T_0 = 102°C$)–target" system is shown in Fig. 4 (curve *2*). This lies much lower than that for the absence of a jet (*1*), which indicates that a proportion of the charged particles in the discharge section is entrained by the jet. We also performed the experiment with a "hotter" air-steam jet with an inlet temperature $T_0 = 200°C$ and no steam oversaturation. It is important to note that the volt-ampere characteristic for this situation almost coincides with that for the electrostatic "capillary-target" system in the absence of a jet.

4. QUALITATIVE ANALYSIS OF THE RESULTS FOR REGIME II

To make qualitative and quantitative estimates, we will consider first the charged drop motion in the space between the capillary and the target in the absence of a jet. The equation of the drop motion with respect to the capillary in the vertical direction z is as follows [9, 10]:

$$\frac{dv}{dt} = g + \frac{QE}{m} - \frac{6\pi r \mu_g v \psi}{m}, \quad \frac{dz}{dt} = v, \quad t=0: \ z=0, \ v=0$$

$$r > 10^{-4} \text{ cm}: \ \psi = 1 + \mathrm{Re}^{2/3}/6, \ \mathrm{Re} = \frac{2r\rho_a v}{\mu_a} \quad (0 \le \mathrm{Re} \le 10^3) \tag{4.1}$$

$$r < 10^{-4} \text{ cm}: \ \psi = (1 + 0.86\mathrm{Kn})^{-1}, \ \mathrm{Kn} = l/r, \ m = 4\pi r^3 \rho/3$$

$$E = \frac{2\varphi(1+\varepsilon)}{H((1+\varepsilon)^2 - (1 - z^0)^2)\ln(1 + 2/\varepsilon)}, \quad z^0 = z/H, \ \varepsilon = 0.01$$

Here, v is the drop velocity in the z direction, H is the distance between the capillary and the target, Kn is the Knudsen number, $l \approx 10^{-5}$ cm is the molecular free path in air, and the subscript a refers to the air parameters. The approximate formula for E is obtained under the assumption that the electric field satisfies the Laplace equation and the capillary surface is approximated by a hyperboloid of revolution [9]. The approximation parameter $\varepsilon = 0.01$ is equal to the ratio of the outer capillary radius to the distance between the capillary and the target. We note that the parameter ε only influences the electric field distribution in a small neighborhood of the capillary end. Thus, a two-fold increase or decrease in ε has almost no impact on E for $z > 0.1$. The quantity ψ is a correction factor for the linear law of spherical particle drag. The first formula for ψ corresponds to the continuum flow regime and the second takes the gas rarefaction effects in the flow around small drops into account; $\mu_a = 2 \cdot 10^{-4}$ g/cm·s.

We determined the drop charge using videophotography with a short exposure time (0.02 s), assuming that the drop radius r is approximately 0.03 cm (according to the data from Fig. 3). By analyzing the vertical traces under the capillary on the stop-images and using Eq. (4.1) for describing the drop motion along the trace, by the shooting method we found that for $\varphi = 15$ kV the ratio of the drop charge to its mass Q/m in the CGS system is approximately 1400 and, hence, $Q = 5.3 \cdot 10^{-11}$ C. This charge is smaller than the limiting charge Q_m (in the Rayleigh criterion, see the first formula in (2.2)) which, for $r = 0.03$ cm, is equal to $1.04 \cdot 10^{-10}$ C. In this case, the electric field generated by the drop charge on the drop surface $E = 53$ kV/cm is smaller than the corona discharge field 110 kV/cm calculated under the assumption that the latter is the same as for an identical metal particle. Lastly, the external electric field at the trace location points is more than an order of magnitude smaller than the critical Taylor field E_* (see Eq. (2.2)). Thus, the drops observed experimentally do not display corona and are stable in the Rayleigh and Taylor criteria, which confirms the possibility of the existence of drops of such size and charge in the interelectrode space.

We will determine the value of the hypothetical current which could be transported only by drops of radius 0.03 cm with the limiting (in the Rayleigh criterion) charge for a given capillary water flow $G = 0.01$ cm^3/s. This current, equal to $8.7 \cdot 10^{-3}$ μA, is almost three orders of magnitude smaller than the volt-ampere characteristic I for the same value of φ, equal to 15 kV, presented in Fig. 5. Hence, in regime II these drops are not the main charge carriers. Within the framework of the aforementioned assumptions, the same conclusion can also be obtained for smaller drops, up to $r = 2$ μm.

On the basis of these estimates, one might suppose that the main charge is carried by even smaller drops with radius $r < 1$ μm. However, the following additional consideration shows that this is also impossible.

Such small drops are almost inertialess and their relaxation times $\tau = m/6\pi\mu_a r\psi$ are very small (see Table 2). The gravity force acting on the drops is much smaller than the electric force. Thus, for $r = 1$ μm, $Q = Q_m$, $\varphi = 15$ kV, and $z^0 = 0.3$ the ratio of these forces $\delta = gm/Q_m E$ is of the order of 10^{-5}. Since $\delta \sim r^{3/2}$, as the drop size decreases, the value of δ becomes even smaller.

With account for our estimates, the equations describing the motion of small (to be specific, positively charged) drops take the form:

$$dz/dt = b^* E_z(x, z), \quad dx/dt = u(x, z) + b^* E_x(x, z), \quad b^* = \frac{Q}{6\pi\mu_a r\psi} \quad (E_x > 0, \quad u + b^* E_x > u) \tag{4.2}$$

Here, the x coordinate is measured along the jet from the capillary section (region $x > 0$ is considered), E_x and E_z are the electric field components in the "capillary-target" system, $u(x, z)$ is the mean velocity distribution in the jet (it is assumed that, in the ambient space, $u = 0$ and the transversal velocity component in the jet is neglected), and b^* is the mobility of the particle carrying the charge Q. The values of b^* calculated using the second formula for ψ from (4.10) on the assumption that $Q = Q_m$ are given in Table 2.

On the range of variation of r in Table 2, the particle mobility variation is small. The value of b^* was determined for the maximum possible charge Q_m. In reality, it is smaller than the values given in Table 2.

The estimates obtained using the system of equations (4.2) show that, after entering the jet, the small drops in Table 2 are fairly intensively entrained in the axial direction and do not reach the target, whose longitudinal dimension measured from the capillary axis is 5 cm. Accordingly, if the current J were carried by these small drops, in the presence of the jet it should decrease. However, the volt-ampere characteristic of the "capillary-hot jet (without condensation)-target" system turned out to be the same as in the "capillary-target" system. This contradiction indicates that, on the range considered, the small drops are not the main charge carriers.

5. REGIME II WITH CONDENSATION IN THE JET

It follows from the estimates given in Section 4 that the main charge carriers must be particles with much greater mobility. Ions are such particles. We give below some arguments in favor of this.

TABLE 2

r, μm	τ, s	b^+, cm²/(V·s)
1	$1.21 \cdot 10^{-5}$	0.578
0.1	$2.1 \cdot 10^{-7}$	0.313
0.01	$1.07 \cdot 10^{-8}$	0.511

The ion mobility is ≈ 2 cm/V·s, which is four times greater than the mobility b^+ given in Table 2. Using Eq. (4.2), it can be shown that in the presence of a jet most ions reach the target. This explains why the currents J in the "capillary-hot jet-target" and "capillary-target" systems are identical.

We performed special experiments in which, in the "capillary-target" system a high voltage was applied to the capillary in the absence of a jet and fluid in the capillary. For $\varphi > 8$ kV, the microammeter registered a current in the target circuit. This current cannot be anything other than the corona discharge current from the capillary. Thus, under the experimental conditions for high φ the ions not directly associated with the presence of the liquid disperse phase are always present in the interelectrode space.

For high φ, ions can appear as a result of microcorona discharges from the surface of a drop formed on the capillary and from the surfaces of drops detached from the capillary.

To prove this statement, we will first obtain an asymptotic dependence of the electric field E_* at an arbitrary point on the corona element on its radius of curvature R as $R \to 0$.

A necessary condition for corona discharge onset is the requirement that in the corona element neighborhood, the electric field **E** reaches a value such that volume ionization of the air molecules by electron impact occurs. Under certain assumptions concerning the interaction between the volume and surface ionization effects, the condition of corona discharge independence can be written in the form [9, 10]:

$$\int_0^s \alpha_{ef}\, ds = K, \qquad \alpha_{ef}(s_0) = 0 \tag{5.1}$$

Here, α_{ef} is an effective ionization coefficient depending on $E = |\mathbf{E}|$, s is the coordinate measured from the surface along a line of force **E**, and s_0 is the boundary of the thin ionization zone adjacent to the corona element. The dependence $\alpha_{ef}(E)$ for air is approximated by the expression [9]:

$$\alpha_{ef} = b(E - E_0)^2 \tag{5.2}$$

Here, b and E_0 are empirical constants. The variation of E near the corona element is attributable mainly to its large curvature and, in the first approximation, can be described by the dependence:

$$E = E_*(1 - s/R), \qquad 1/R = 1/R_1 + 1/R_2 \tag{5.3}$$

Here, E_* is the field at the considered point of the corona element surface (corona discharge ignition field), and R_1 and R_2 are the main curvatures at this point. After substitution of Eqs. (5.2) and (5.3) in (5.1), we obtain the following equation for determining E_*:

$$\frac{(q-1)^3}{q} = \frac{3K}{bE_0^2 R}, \quad q = E_*/E_0, \quad R \to 0: \quad E_*/E_0 \approx \left(\frac{3K}{bE_0^2}\right)^{1/2} R^{-1/2} \tag{5.4}$$

The last formula in (5.4) is the required asymptotic estimate. On the basis of the data from [9, 10], we can assume that $K = 8.45$, $b = 0.2$ cm/(kV)², and $E_0 = 24$ kV/cm. We will use the asymptotic formula obtained for predicting corona formation from small drops. Assuming that the drop charge is maximum Q_* so that the electric field on the drop surface is $E_m = Q_m/r_2$ and using Eqs. (2.2) and (5.4), we obtain: $E_m/E_* = 1.6$. To obtain this estimate we used the values of the constants K, b, and E_0 given above. The water surface tension α was taken equal to 72 dyne/cm. Essentially, in the aforementioned approximation for small drops the ratio E_m/E_* is independent of the drop size.

The estimate obtained shows that small drops with the maximum (in the Rayleigh criterion) charge Q_m can display a corona and generate ions. Certainly, in reality the drop charge may be much smaller, for liquid drops the values of the constants may differ from those used and the possibility of corona discharge from the drop surface needs to be specially discussed in each particular case.

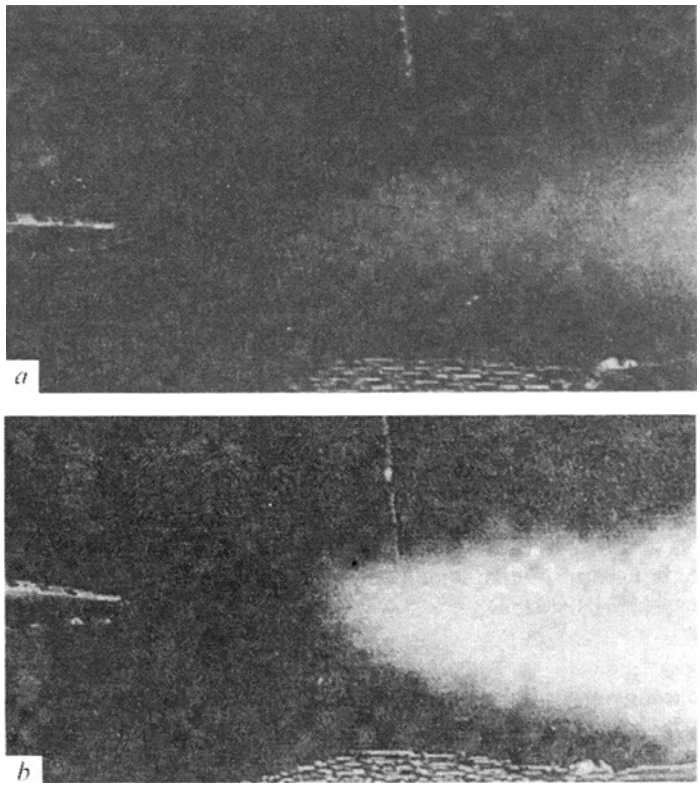

Fig. 6. Condensation zones in the air-steam jet for a capillary potential $\varphi = 12$ kV (a – grounded nozzle; b – identical capillary and nozzle potentials).

We note that the aforementioned possibility of corona discharge from small drops does not change the conclusion reached above that such drops cannot be the main charge carriers. Indeed, corona formation from the drops results in a decrease in their charge and hence a decrease in the drop mobility and an increase in the drop displacement Δr along the jet. This makes drop impingement on the target even more impossible.

The presence of the ions in the interelectrode space explains the main experimental result, namely, (i) the appearance for $\varphi > 8$ kV of a long condensation region in the air-steam jet ($T_0 = 102°C$) located between the capillary and the target and (ii) a decrease in the current J in the presence of a jet as compared with the case when the jet is absent. We recall that in the absence of a capillary system there is no condensation in the jet despite the existence of oversaturation zones in it. On the ions entering the jet nucleation develops [3, 13]. The nucleation centers with an initial size of ~10 nm increase in size due to steam condensation on them and are transformed into drops which form a visible condensation zone (see Fig. 5). Under the experimental conditions, the drop radius growth rate is $\sim 10^{-1}$ cm/s and, as the drops travel in the jet, their size reaches the value ~ 1 μm. When these drops carry a small charge, they travel downstream without velocity slip with the jet. If the drop charge becomes substantial (due to inductive drop charging in the electric field in the presence of surrounding ions) and even attains the limiting value Q_m, then, as shown at the end of Section 4, the drops cannot reach the target. The existence of this ion "sink" in the jet explains the decrease in the current on the target when condensation develops. This again confirms the conclusion that the main charge carriers are the ions. We will now comment on the condensation zone shape shown in Fig. 5. The visible condensation zone begins at a point A located upstream of the capillary section. This is connected with the fact that, as a result of the development of instabilities and the action of the forces pushing the particles apart, the charged particles occupy a certain space of approximately conical shape between the capillary and the jet. As a result, the ions enter the flow upstream of the capillary section where the "electric" condensation starts. The drops formed on the ions are removed downstream by the jet and occupy almost the entire jet section. The latter can be explained in terms of the passive admixture diffusion mechanisms in a turbulent flow.

One more convincing indication of the presence of ions in the interelectrode space is the experiments carried out for an initial steam jet temperature $R_0 = 102°C$ with a grounded steam nozzle. In this case, due to the existence of a potential difference between the capillary and the nozzle ions with high mobility, located in the space between the capillary and the jet and also in the low-velocity part of the jet, can move toward the nozzle. A portion of the ions enters the nozzle directly.

The other ions, entering the steam oversaturation region, become condensation centers and the drops formed on them are removed downstream. This situation is shown in Fig. 6*a*. For comparison, Fig. 6*b* shows the case when the capillary and the nozzle had identical potentials. In Fig. 6*a*, the visible condensation zone length is greater because the "electric condensation" starts much closer to the nozzle and is less intense since some of the ions impinge directly on the nozzle surface.

Summary. The interaction between an electrically charged liquid-drop phase and an air-steam turbulent jet is investigated experimentally in a specially designed setup consisting of a drop generator, an air-steam jet, and an electrical system. The main components of the drop generator located outside the jet are a flow rate controller and a capillary under a potential difference φ which can attain values of 20 kV. The air-steam turbulent jet is created by steam flowing out from a nozzle into the ambient air at various nozzle outlet steam temperatures T_0. In the basic regime ($T_0 = 102°C$), when the jet mixes with fairly cold ambient air, steam oversaturation conditions are attained in it, but in the absence of a drop generator the oversaturation level is insufficient for the development of homogeneous condensation.

Two regimes of interaction between the electrically charged drops and the jet realized for $\varphi < 8$ kV and for 8 kV $< \varphi <$ 20 kV, respectively, are considered. The first (regime *I*) is characterized by regular drop launching from the capillary and drop transformation into small charged clusters without the development of condensation in the jet and also by a very small current (small fractions of a μA) in the "capillary-target" system. The drop parameters (electric charge, size, succession frequency) were determined by direct optical and electrical measurements. The modeling of the motion of discrete charged clusters in aircraft engine jets is realized in regime I.

The essentially different regime II (realized for high potential differences) is characterized by irregular drop launching from the capillary, a sharp increase in the current on the target (up to 5 μA), and the formation of a long condensation zone in the jet, starting upstream from the vertical axis of the capillary.

A system of proofs of the fact that, in regime II, the electric current is mainly an "ion current" is proposed. The ions are formed in the corona discharge (i) from the drops formed at the capillary end and located in the discharge space and also (ii) directly on the capillary surface. In the air-steam jet, nucleation starts precisely on the ions, then the nuclei grow and are removed downstream by the jet.

To prove the possibility of corona formation on small drops, the theory of the corona discharge ionization zone is used and a generalizing asymptotic formula is obtained for the electric corona discharge ignition field at an arbitrary point of a surface of large curvature.

Regime II made it possible to realize the situation in which, in the turbulent jet, there are (i) continuously distributed small charged liquid drops formed as a result of nucleation on ions and traveling without velocity slip with the jet and also (ii) larger original charged drops which discretely occupy the jet volume. This is very important for modeling the electrical processes in engine jets.

The work received financial support from the Russian Foundation for Basic Research (project No. 99-01-00983).

REFERENCES

1. R. P. Couch, "Detecting abnormal turbine engine deterioration using electrostatic methods," AIAA Paper no. 78–1473 (1977).
2. A. B. Vatazhin, D. A. Golentsov, V. A. Likhter, and V. I. Shul'gin, "The problem of contactless electrostatic diagnostics of aircraft engine conditions. Theoretical and bench modeling," *Izv. Ross. Akad. Nauk. Mekh. Zhidk. Gaza*, no. 2, 83 (1997).
3. A. Vatazhin, A. Lebedev, V. Likhter, V. Shul'gin, and A. Sorokin, "Turbulent air-steam jets with a condensed dispersed phase: Theory, experiment, numerical modeling," *J. Aerosol Sci.*, **26**, no. 1, 71 (1995).
4. G. Taylor, "Disintegration of water drops in an electric field," *Proc. Roy. Soc. London. Ser. A*, **280**, no. 1382, 383 (1964).
5. A. M. Gannan-Calvo, J. Dàvala, and A. Barrero, "Current and droplet size in the electrospraying of fluids. Scaling laws," *J. Aerosol Sci.*, **28**, no. 2, 249 (1997).
6. L. T. Cherney, "Structure of Taylor cone-jets: Limit of low flow rates," *J. Fluid Mech.*, **378**, 167 (1999).
7. J. W. Rayleigh, "On the equilibrium of liquid conducting masses charged with electricity," *Phil. Mag.*, **14**, 184 (1882).
8. A. I. Grigor'ev and O. A. Sinkevich, "Towards a mechanism of the development of liquid drop instability in an electric field," *Izv. Akad. Nauk SSSR, Mekh. Zhidk. Gaza*, no. 6, 10 (1985).
9. I. P. Vereshchagin, V. I. Levitov, G. Z. Mirzabekyan, and M.M. Pashin, *Fundamentals of Dispersed-System Electrogasdynamics* [in Russian], Energiya, Moscow (1974).
10. A. B. Vatazhin, V. I. Grabovskii, V. a. Likhter, and V. I. Shul'gin, *Electrogasdynamical Flows* [in Russian], Nauka, Moscow (1983).
11. A. Jaworek and A. Krupa, "Generation and characteristics of the procession mode of EHD spraying," *J. Aerosol Sci.*, **27**, no. 1, 75 (1996).
12. Ya. E. Geguzin, *Droplet* [in Russian], Nauka, Moscow (1973).
13. A. B. Vatazhin, V. A. Likhter, a. a. Sorokin, and V. I. Shul'gin, "Corona discharge in an air-steam jet with condensation. Stationary and pulsatory characteristics," *In: turbulent Jet Flows with Condensation and Electrophysical Effects. V.1*, Trudy TsIAM, no. 1288, 110 (1991).